

# Temperature Dependence of the Relaxation Rates of $\alpha$ and $\delta$ Relaxation in Liquid-Crystalline Side-Group Polymethacrylates

A. Schönhals,<sup>\*,†,‡</sup> D. Wolff,<sup>‡</sup> and J. Springer<sup>‡</sup>

Bundesanstalt für Materialforschung und -prüfung, Unter den Eichen 87, Fachgruppe VI.3, D-12205 Berlin, Germany, and Institut für Technische Chemie, Technische Universität Berlin, Strasse des 17. Juni 135, D-10623 Berlin, Germany

Received October 20, 1997; Revised Manuscript Received August 18, 1998

**ABSTRACT:** Dielectric spectroscopy in the frequency range from  $10^{-2}$  to  $10^6$  Hz and in the temperature range from 190 to 430 K is employed to analyze the temperature dependence of the relaxation rates of the  $\alpha$  and  $\delta$  relaxation of liquid-crystalline polymethacrylates having derivatives of (*p*-alkoxyphenyl)-benzoate as mesogenic units in the side group. Different mesophases were achieved by variation of the spacer length. When a temperature derivative method was applied, it was found that the temperature dependence of the relaxation rate of the dielectric  $\alpha$  relaxation in these systems displays two different regions: an Arrhenius-like behavior at high temperatures and a behavior according to the Vogel–Fulcher–Tammann law at low temperatures which is characteristic for the dynamic glass transition in general. The crossover between these two dependencies characterized by a temperature  $T_{dc}$  is shifted to lower temperatures with increasing spacer length, but the ratio of  $T_{dc}$  and the glass transition temperature is nearly independent of the spacer length. The result is discussed in the framework of the cooperativity of the glass transition. The ratio of the relaxation rates of the  $\alpha$  and  $\delta$  processes increases with decreasing temperature in the liquid-crystalline mesophase range. This is explained by an increase of local order with decreasing temperature. Close to the glass transition temperature, the ratio of the relaxation rates of the  $\alpha$  and  $\delta$  processes decreases. This indicates that the dielectric  $\alpha$  and  $\delta$  processes freeze at least together and cannot be regarded further as independent relaxation processes in that temperature regime.

## 1. Introduction

It has been proved by numerous studies<sup>1</sup> that dielectric relaxation spectroscopy is a useful tool to study the molecular dynamics of polymeric systems. This method provides direct information about the molecular dynamics of dipole moments related to the polymer chain or parts of it. Moreover, information on the structure or micromorphology of the system under investigation can be indirectly obtained because the motional processes depend on it. In that case the motion of dipoles is taken as a probe for structure. These considerations are also true for polymeric liquid crystals, which have received much attention since their first synthesis<sup>2,3</sup> as advanced materials for various applications because of their multifunctional character. In side-group polymeric liquid crystals (SGPLC) the mesogenic unit is located in a side group of the polymer backbone, and it is expected that such materials can be applied as active components for optical data storage, holographic applications, and electro-optical devices. This was demonstrated by Wendorff and co-workers<sup>4</sup> for the first time. In these materials molecular dynamics—which can be studied by dielectric spectroscopy—is contemporary and important for their application because the storage of information is linked to a reorientation of molecules or parts of it.

Dielectric investigations on side-group polymeric liquid crystals were carried out by Kresse and co-workers<sup>5–7</sup> the first time followed by the work of Haase and co-workers,<sup>8,9</sup> Williams and his group,<sup>10</sup> and Kremer et al.<sup>11</sup> where the latter focus mainly on ferroelectric systems. A number of reviews are also available.<sup>12–15</sup>

Because of the different possibilities of dipole reorientation in side-group polymeric liquid crystals, several dielectric active relaxation processes can be observed. Zentel et al.<sup>16</sup> have set up an appropriate nomenclature for unoriented systems. At low temperatures the rotational fluctuations of the tail groups and of the spacer groups can be observed and are called  $\gamma_1$  and  $\gamma_2$  processes. With increasing temperature, these processes are followed by the so-called  $\beta$  relaxation that was assigned to rotational fluctuation of the mesogenic group around its long axis. It was shown that the temperature dependence of the relaxation rate is mainly given by the actual mesophase structure.<sup>15,17–19</sup>

At even higher temperatures than those of the  $\beta$  relaxation, a further relaxation process can be observed and is called  $\alpha$  relaxation. The temperature dependence of the relaxation rate of the  $\alpha$  relaxation is complicated and shows for polymers having a derivative of phenylbenzoate as the mesogenic unit in the side group a curved trace versus reciprocal temperature.<sup>16,18</sup> Moreover, at low frequencies the temperature of maximal loss of the  $\alpha$  relaxation seems to agree with the glass transition temperature  $T_g$  which can be measured by calorimetric methods.<sup>16,18</sup> Therefore, the  $\alpha$  relaxation is related to the dynamic glass transition of the system.<sup>16</sup> On the other hand, it should be noted that Williams and co-workers<sup>20,21</sup> have assigned the  $\alpha$  relaxation to rotational fluctuations of the transversal dipole moment of the mesogenic unit. This assignment resulted from experiments on oriented polysiloxanes having a strong dipole moment in the side group but a very weak one in the polymeric backbone. One of the main purposes of that contribution is to analyze the temperature dependence of the relaxation rate of the  $\alpha$  relaxation in detail by applying a new derivative technique.<sup>22</sup> It

<sup>†</sup> Bundesanstalt für Materialforschung und -prüfung.  
<sup>‡</sup> Technische Universität Berlin.

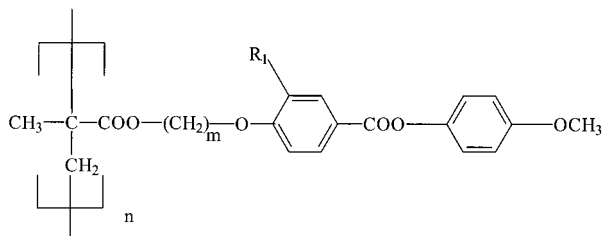


**Figure 1.** Structure of the repeating unit of the polymers studied.

should be noted that the glass transition itself is even for low molecular weight glass-forming systems and amorphous polymers an actual but unsolved problem of solid-state physics.<sup>23,24</sup>

At even higher temperatures (or at even lower frequencies) than those of the  $\alpha$  relaxation, a further relaxation process called  $\delta$  relaxation can be detected. The  $\delta$  relaxation seems to be characteristic for side-group liquid polymeric crystals. Detailed investigations have shown that this relaxation process is related to rotational fluctuations of the dipole component which is parallel to the mesogenic side group about the local director axis.<sup>9,20,21</sup> In that contribution also the temperature dependence of the relaxation rate of the  $\delta$  process is analyzed and compared to that of the  $\alpha$  relaxation.

The theory of the dielectric behavior of aligned nematic liquid-crystalline side-group polymers was mainly developed by Attard and Williams.<sup>20,21</sup> This treatment is based on the Maier-Saupe treatment<sup>25</sup> and on the Nordio-Rigatti-Segre theory<sup>26</sup> of dielectric relaxation of nematic low molecular mass liquid crystals. A review can be found in Moscicki's work.<sup>13</sup> A starting point is the consideration that each mesogenic unit has two components of its molecular dipole vector longitudinal and transverse to its long axis. Dielectric relaxation proofs dipole fluctuations which are in parallel to the outer electric field vector. The orientation of simple liquid-crystalline phases like nematics can be described by the nematic director,<sup>27</sup> which is related to the macroscopic director order parameter  $S$ . Therefore, the complex dielectric function  $\epsilon^*$  should have two main components  $\epsilon^*$ , and  $\epsilon^*_{\perp}$  (different from zero) which are parallel and perpendicular to the nematic director. Clearly, both of these components of the dielectric function depend on the order parameter  $S$  and so dielectric behavior of the macroscopic sample depends on the alignment conditions. From a microscopic point of view the dielectric behavior is described by correlation functions of the polarization fluctuations parallel and perpendicular to the nematic director. These can be expressed by four orthogonal dielectric modes given by correlation functions of the longitudinal and transverse component of the molecular dipole vector projected parallel and perpendicular to the nematic director. Also the dielectric intensities are predicted by the theory.

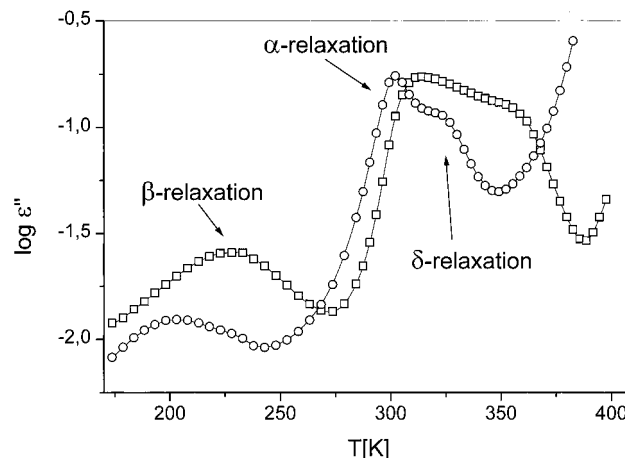
## 2. Experimental Section

Figure 1 and Table 1 define the structure of the repeating unit of the investigated polymethacrylates. Derivatives of ( $\rho$ -alkoxyphenyl)benzoate were used as mesogenic units in the side groups. To achieve different mesophases, the number of the methylene spacer groups was varied. Some details of the synthesis and of the chemical characterization can be found in ref 28. The thermal behavior was determined by DSC, and the phase characterization was done by X-ray measurements.<sup>29</sup> The values of the glass transition temperature  $T_g$ , the phase transition temperatures, and the type of the liquid-crystalline

**Table 1. Chemical Structure and Transition Temperatures of the Investigated Polymers (see Figure 1)<sup>a</sup>**

code	n	R <sub>1</sub>	T <sub>g</sub> [K]	phase transition temp [K]	T <sub>dc</sub> [K]	T <sub>dc</sub> /T <sub>g</sub>
P2	2	H	370	N 394 I		
P4	4	H	333	N 377 I	370	1.11
P6	6	H	314	S <sub>A</sub> 342 N 383 I	366	1.15
P8	8	H	307	S <sub>A</sub> 367 N 394 I	339	1.10
P10	10	H	289	S <sub>A</sub> 393 I	320	1.11
P12	12	H	289	S <sub>A</sub> 396 I	315	1.09
P-iso	6	OCH <sub>3</sub>	322	I		

<sup>a</sup> I = isotropic state; N = nematic mesophase; S<sub>A</sub> = smectic A mesophase; T<sub>dc</sub> is a characteristic temperature (for the definition see the Results and Discussion section). For samples P2 and P-iso no characteristic temperature could be estimated for different reasons (see the Results and Discussion section).



**Figure 2.** log  $\epsilon''$  versus temperature at fixed frequencies for the sample P10:  $\circ$ , 147 Hz;  $\square$ , 1000 Hz.

phase are collected in Table 1. In order to investigate also a structurally similar material which does not show a macroscopic liquid-crystalline behavior, the hydrogen in the meta position of the benzoate ring was substituted by a methoxy group. The corresponding data are also listed in Table 1.

The procedure for the dielectric measurements has been described elsewhere.<sup>17</sup> The samples were pressed between gold-plated stainless steel electrodes at a temperature of 423 K where the spacing of the electrodes of  $50 \pm 1 \mu\text{m}$  was maintained by fused silica fibers. The dielectric properties

$$\epsilon'(f) = \epsilon'(f) - i\epsilon''(f) \quad (1)$$

( $f$  = frequency,  $\epsilon'$  = real part,  $\epsilon''$  = imaginary part,  $i = \sqrt{-1}$ ) were measured by a Schlumberger frequency-response analyzer FRA 1260 coupled to a buffer amplifier of variable gain<sup>30</sup> (Chelsea Dielectric Interface). The temperature of the sample was controlled by a custom-made nitrogen gas jet heating system with a resolution of  $\pm 0.02$  K. The sample was thermally equilibrated at the selected temperature, and then an isothermal frequency scan was done. All samples were measured in a nominal unaligned state. It should be noted that the procedure of sample preparation can align the material to some extent. Because the  $\delta$  process is mainly due to the dipole moment which is in parallel to the mesogenic unit, an alignment can change the relative dielectric strength of that process compared to the  $\alpha$  relaxation.<sup>20,21</sup> Measurements on aligned samples are in preparation.

## 3. Results and Discussion

Figure 2 shows the dielectric loss  $\epsilon''$  versus temperature at two fixed frequencies for the polymer P10. A comparison of the dielectric loss of the liquid-crystalline sample P6 and the sample which shows no liquid-

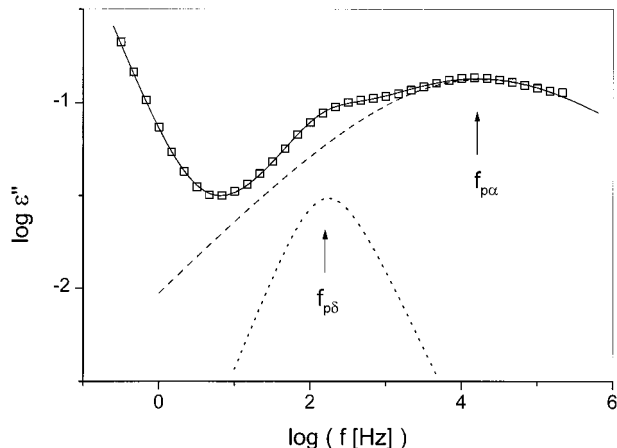


**Figure 3.** Example for the fitting procedure for the polymer P8 at 352.3 K: dashed line,  $\alpha$  relaxation ( $\beta = 0.408$ ,  $\gamma = 0.736$ ,  $\log f_0 = 3.94$ ,  $\Delta\epsilon = 0.897$ ); dotted line,  $\delta$  process ( $\beta = 1$ ,  $\gamma = 0.853$ ,  $\log f_0 = 2.18$ ,  $\Delta\epsilon = 0.06$ ); solid line, whole fitting function including the conductivity contribution.

crystalline behavior is given elsewhere.<sup>31</sup> As was pointed out, at low temperatures the  $\beta$  relaxation takes place followed by the  $\alpha$  and  $\delta$  processes at higher temperatures. As is usual, the loss peaks shift to higher temperatures as frequency increases. An analysis of the dependence of the  $\beta$  relaxation recently has been presented for this set of liquid-crystalline side-group polymers.<sup>17,18</sup> So, this paper concentrates on the detailed discussion of the temperature dependence of the relaxation rates of the  $\alpha$  and  $\delta$  processes. To analyze the temperature dependence of the relaxation rate at maximal loss  $f_{p\alpha}$  for both relaxation processes, an evaluation method<sup>32</sup> based on the model function of Havriliak and Negami (HN function)<sup>33</sup> is applied. Because  $\alpha$  and  $\beta$  relaxations are strongly overlapped, the  $\alpha$  relaxation has to be separated from the  $\delta$  process. For that reason two HN functions are fitted simultaneously to the isothermal data

$$\epsilon'(f) - \epsilon_\infty = \sum_k \frac{\Delta\epsilon_k}{(1 + (if/f_{0,k})^{\beta_k})^{\gamma_k}} \quad (2)$$

where  $k = \alpha$  and  $\delta$ . For each process  $\Delta\epsilon$  is the intensity or dielectric relaxation strength and  $f_0$  is a characteristic frequency which is nearly equal to the peak frequency  $f_p$ .  $\beta$  and  $\gamma$  denote fractional shape parameters ( $0 < \beta \leq 1$  and  $0 < \beta\gamma \leq 1$ ) due to the symmetric or asymmetric broadening of the loss peak.  $\epsilon_\infty$  is  $\epsilon'(f)$  for  $f \gg f_{p\alpha}$ . The term  $C/\sigma$  describes the conductivity contribution.  $C$  is directly related to the dc conductivity, where  $\sigma$  is a fitting constant. For pure ohmic contacts and no Maxwell-Wagner processes,  $\sigma = 1$  holds. Experimentally,  $0.5 < \sigma \leq 1$  was found. To reduce the number of free fit parameters,  $\beta_\delta$  was kept fixed at 1 because it was known that the  $\delta$  relaxation corresponds more or less to a Debye process.<sup>21,34</sup> Figure 3 shows an example of the fits for the polymer P8, and Figure 4 displays the temperature dependences of the relaxation rates for all three process for the sample P10. The temperature dependence of the relaxation rate of the  $\beta$  relaxation shows an Arrhenius-like behavior. The dependence of the activation parameters on the mesomorphic structure is extensively discussed in refs 17, 18, and 31. The dependence of the relaxation rates for the  $\alpha$  and  $\delta$  processes is complicated and will be analyzed in this

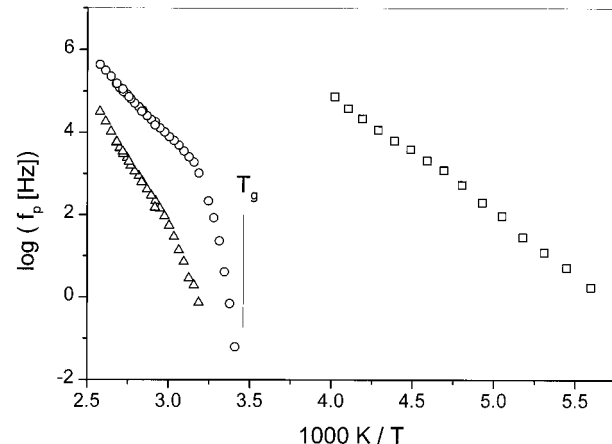


**Figure 4.** Temperature dependence of the relaxation rates for the  $\beta$  (□),  $\alpha$  (○), and  $\delta$  (△) processes for the polymer P10.

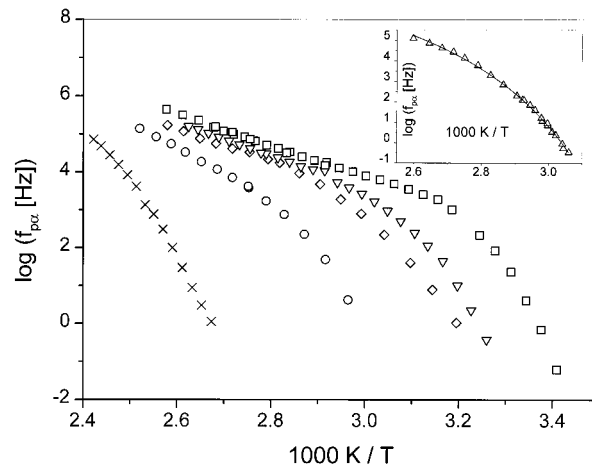


**Figure 5.**  $\log f_{p\alpha}$  versus  $1000/T$  for the different liquid-crystalline samples:  $\times$ ,  $n = 2$ ;  $\circ$ ,  $n = 4$ ;  $\diamond$ ,  $n = 6$ ;  $\nabla$ ,  $n = 8$ ;  $\square$ ,  $n = 10$ . The inset shows the same for the isotropic sample P-iso ( $\triangle$ ), where the line is a fit of the VFT equation to the data.

paper. Figure 4 shows further that the temperature dependences of the relaxation rates for both processes are different.

**α Relaxation.** The logarithm of the relaxation rates for the  $\alpha$  process,  $\log f_{p\alpha}$ , is plotted versus  $1/T$  in Figure 5 for the liquid-crystalline samples. The inset of Figure 5 shows the same for the isotropic sample. The temperature dependence of  $f_{p\alpha}$  of the sample P-iso shows a behavior which is characteristic for amorphous polymers. This means the temperature dependence of  $f_{p\alpha}$  can be described by the well-known Vogel-Fulcher-Tamman (VFT) equation<sup>35</sup>

$$\log f_p = \log f_\infty - \frac{A}{(T - T_0)} \quad (3)$$

In eq 3,  $A$  is a constant,  $\log f_{p\infty}$  is a characteristic frequency if  $T$  approaches infinity, and  $T_0$  is the so-called Vogel or ideal glass transition temperature. In contradiction to that for the liquid-crystalline samples, the temperature dependence of  $\log f_{p\alpha}$  is very complicated. At low temperatures  $\log f_{p\alpha}$  shows a curved trace versus  $1/T$  whereas at high temperatures  $f_{p\alpha}$  seems to follow an Arrhenius law

$$f_p = f_\infty \exp[-E_A/kT] \quad (4)$$

where  $f_\infty$  is a prefactor and  $E_A$  is the activation energy

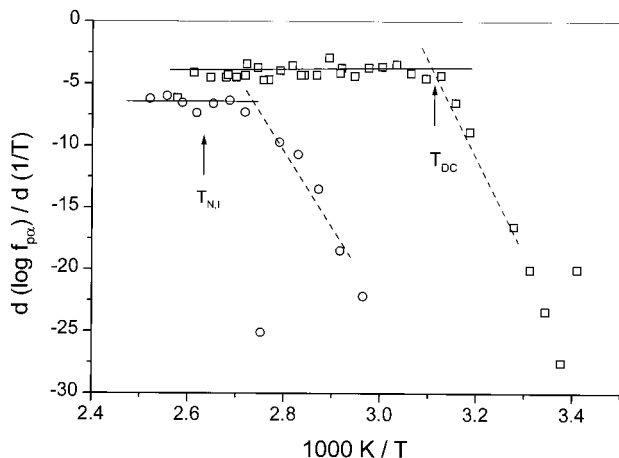


**Figure 6.**  $d(\log f_{pa})/d(1/T)$  versus  $1/T$  for the polymers P4 (○) and P10 (□). The solid lines are the average values in the high-temperature range where the dashed lines are a guide for the eyes. The intersection of both lines defines a characteristic temperature  $T_{dc}$ . Because of the derivation process, the data show a relatively large scatter.

( $kT$  has the usual meaning). The crossover from the high-temperature behavior to the low-temperature one seems to shift to lower temperature with increasing spacer length.

To analyze the temperature dependence of  $f_{pa}$  in more detail, a temperature derivative method<sup>22</sup> developed recently is applied. This method is extremely sensitive to differences in the functional form of  $f(T)$ , irrespective of the offsets in the prefactors. For a functional dependence according to an Arrhenius equation, one gets

$$\frac{d \log f_{AHR}}{d(1/T)} = - \frac{E_A}{\ln(10)k} \quad (5)$$

whereas for a behavior according to the VFT equation

$$\left[ \frac{d \log f_{VFT}}{dT} \right]^{-1/2} = A^{-1/2} (T - T_0) \quad (6)$$

holds.

In Figure 6  $d(\log f_{pa})/d(1/T)$  is plotted versus reciprocal temperature for the polymers P4 and P10. This plot shows that at high temperatures the temperature dependence of the relaxation rate of the  $\alpha$  relaxations follows an Arrhenius-like behavior. If temperature decreases, the temperature dependence of  $f_{pa}$  changes from that of Arrhenius-like behavior to a different temperature dependence which will be discussed later. From the average value at high temperatures, a corresponding apparent activation energy can be estimated according to eq 5 for each spacer length. Figure 7, where  $E_A$  is plotted versus spacer length, shows that  $E_A$  decreases with increasing spacer length. (For  $n = 2$ , no Arrhenius-like region could be detected.) It should be noted that the estimated values are much too high for local molecular processes, particularly for short spacer lengths.

The low-temperature behavior can be approximated by a straight line. From the intersection of this line with the high-temperature Arrhenius-like behavior, a characteristic temperature  $T_{dc}$  can be defined. With increasing spacer length,  $T_{dc}$  decreases, as is shown by the inset of Figure 7. It has to be mentioned that in no case does  $T_{dc}$  agree with a phase transition temperature in the system. This becomes especially clear for the systems

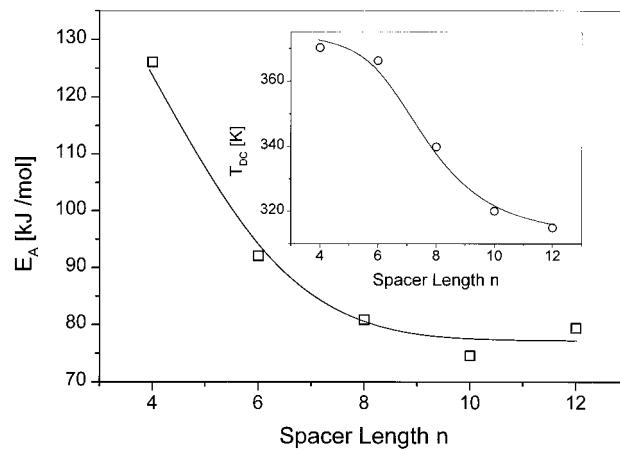


**Figure 7.** Apparent activation energy for the high-temperature range versus spacer length  $n$ . The inset gives the characteristic temperature  $T_{dc}$  also versus spacer lengths. Lines are guides for the eyes.

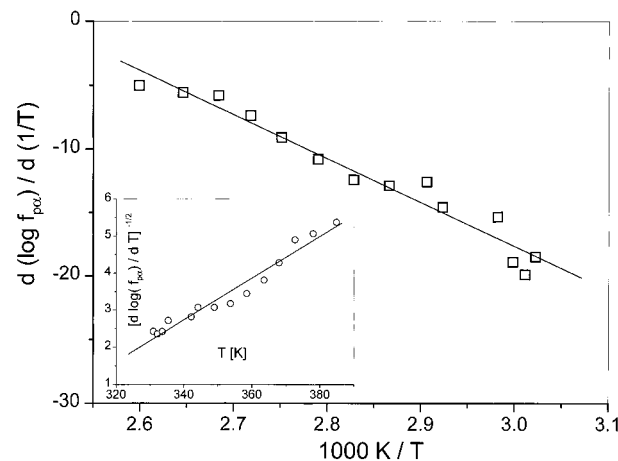


**Figure 8.**  $d(\log f_{pa})/d(1/T)$  versus  $1/T$  for the polymer P-iso. The inset shows  $[d \log f_{pa}/dT]^{-1/2}$  versus temperature.

with longer spacers, for instance,  $n = 10$  and  $n = 12$ , where the phase transition temperatures are out of the measured temperature window. To compare the dynamic behavior of the different samples irrespective of their glass transition temperature, the ratio  $T_{dc}/T_g$  is calculated. Table 1 shows that  $T_{dc}/T_g$  has approximately a constant value for the investigated homologous polymers. This gives evidence that  $T_{dc}$  should be related to the glass transition of the system.

In contradiction to the behavior of the liquid-crystalline polymers, the isotropic sample shows a quite different behavior. Figure 8 gives  $d(\log f_{pa})/d(1/T)$  versus reciprocal temperature for that sample. There is no constant value of this quantity at high temperatures. In the whole temperature range investigated  $d(\log f_{pa})/d(1/T)$  decreases with decreasing temperature. In the inset of Figure 8, a plot according to eq 6 is given. This plot shows that for the isotropic material  $f_{pa}$  can be described in the whole temperature range by the VFT equation.

According to eq 6, in Figure 9  $[d \log f_{pa}/dT]^{-1/2}$  is plotted versus temperature. This plot shows that the low-temperature behavior can be approximated by a straight line. This means that at lower temperature than  $T_{dc}$   $f_{pa}$  varies with temperature according to the VFT equation (see eq 6). When a linear equation is fitted to the data, both VFT parameter  $A$  and the Vogel temperature  $T_0$  can be estimated. Figure 10 shows that  $A$

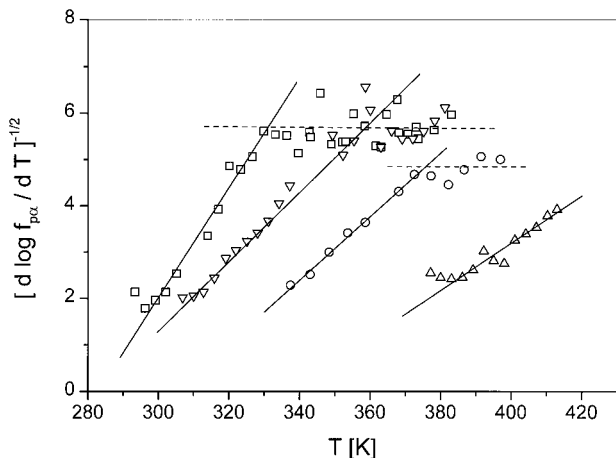


**Figure 9.**  $[d \log f_{\alpha} / d T]^{-1/2}$  versus temperature for the liquid-crystalline polymers:  $\triangle$ ,  $n = 2$ ;  $\circ$ ,  $n = 4$ ;  $\nabla$ ,  $n = 8$ ;  $\square$ ,  $n = 10$ . (The spacer lengths  $n = 6$  and  $n = 12$  are omitted for the sake of clarity.) The solid lines are linear fits to the low-temperature data. The dashed lines are guides for the eyes.

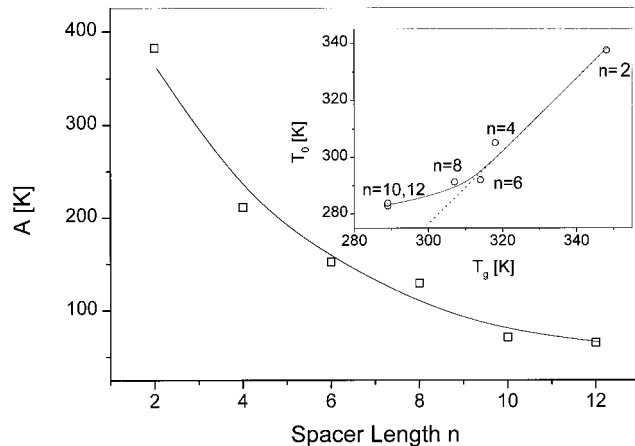


**Figure 10.** VFT parameter  $A$  versus spacer length  $n$ . The inset shows  $T_0$  versus  $T_g$ . Lines are guides for the eyes.

decreases with increasing spacer length and seems to approach a constant value above the spacer lengths  $n = 10$  and  $n = 12$ . The inset of Figure 10 gives the Vogel temperature  $T_0$  versus the glass transition temperature  $T_g$  measured by calorimetric methods. For short spacer lengths there seems to be a one-to-one relationship of both quantities, as is found for amorphous systems. For long spacer lengths again a bend to constant value is observed.

The main dipole moment in the system is due to the mesogenic unit. However, there is also an ester group which carries a dipole moment. This fact was considered by Haase et al., who added an additional dipole moment because of the ester group.<sup>8,9</sup> The  $\alpha$  relaxation in these liquid-crystalline polymethacrylates was related to the dynamic glass transition of the system, which is due to segmental dynamics. This conclusion is supported by the correlation of  $T_0$  with  $T_g$ . However, the molecular dynamics in conventional poly(*n*-alkyl methacrylate)s is still a subject of discussion.<sup>36–38</sup> Besides the strong plasticization effect which increases with increasing spacer length,<sup>39</sup> a strong broadening of the thermal glass transition range also has been found with increasing lengths of the *n*-alkyl side group.<sup>40</sup> Although the glass transition is not completely understood in general up to now, there seems to be only little doubt that the glass transition is a cooperative process where the cooperat-

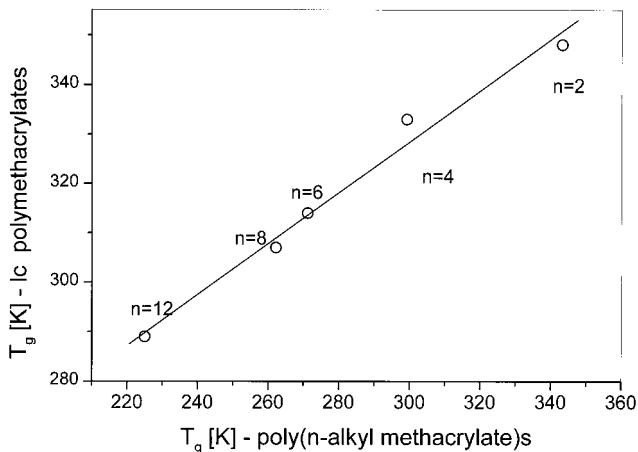


**Figure 11.** Glass transition temperature of liquid crystalline (lc) polymethacrylates versus glass transition temperature of poly(*n*-alkyl methacrylate)s. The solid line is the linear regression through all data points.

ivity sets in at temperatures well above  $T_g$  and that the extent of the cooperativity increases with decreasing temperature. Particularly for conventional poly(*n*-alkyl methacrylate)s, it has been found that this onset of the glass transition, first, is closer to  $T_g$  than that for other materials and, second, is shifted to lower temperatures (compared to the respective  $T_g$ ) with increasing number of alkyl units in the side group.<sup>40</sup> Moreover, the spacial extent of cooperativity at  $T_g$  is rather small for these materials and decreases also with the number of alkyl units. It is also known for poly(*n*-alkyl methacrylate)s that the dielectric relaxation behavior in the high-temperature region down to relative low temperatures (compared to other polymers) is mainly determined by a so-called  $(\alpha\beta)$  process whose relaxation rate shows an activated temperature dependence.<sup>36,40</sup>

This line of argument is used to discuss the  $\alpha$  relaxation for the liquid-crystalline systems. As was pointed out, the correlation of  $T_0$  and  $T_g$  supports the fact that the  $\alpha$  relaxation is related to the glass transition in these systems. Also the apparent activation energy in the high-temperature range is much too high for true local processes. To discuss the glass transition in liquid-crystalline side-group polymers, the micromorphology of liquid-crystalline side-group polymers has to be considered first. At temperatures above the clearing temperature, the mesogenic units are distributed randomly. If the temperature decreases and the system undergoes a phase transition, the mesogens are organized in a layer-like structure, and backbone-segment-rich and spacer-rich regions remain within this layer-like structure. According to Lipatov,<sup>41</sup> this can be interpreted as a kind of microphase separation. So, the structure of bulk liquid-crystalline side-group polymers can be regarded as microbiphasic to some respect consisting of locally layer-like structures with a high concentration of mesogens and a second polymer backbone- and spacer-rich microphase. The glass transition is related to the latter one. Although the conventional poly(*n*-alkyl methacrylate)s and the investigated systems are quite different, the rough correlation of the glass transition temperatures of both systems displayed in Figure 11 endorses this statement. With increasing spacer length, the relative volume of the backbone- and spacer-rich microphase, which is called the “quasi isotropic microphase” here, increases. Moreover, the layer-like structures can be regarded as a kind of

geometrical confinement for this phase. This means further that for longer spacers and particularly at high temperatures the molecular motions in the quasi isotropic microphase should become more and more similar to those of the corresponding poly(*n*-alkyl methacrylate)s. For shorter spacers the molecular motions in the quasi isotropic microphase will be influenced more and more by the layers. For that reason the apparent activation energy for the high-temperature range increases with decreasing spacer length (see Figure 6). Consider now a fixed spacer length, for instance,  $n = 10$ . At high temperatures the degree of cooperativity is small, and therefore the corresponding molecular motions are not influenced so much by the layers. With decreasing temperature, the spacial extent of cooperativity increases and, at a certain point, the molecular motions responsible for the  $\alpha$  process will be influenced by the layer structure, which acts as a kind of geometrical confinement. At this point marked by the temperature  $T_{dc}$ , the kind of molecular motion changes. So,  $T_c$  is due to a dynamical process and has nothing to do with a phase transition. Because the volume of the quasi isotropic microphase increases with increasing spacer length  $n$ ,  $T_{dc}$  shifts to lower temperatures with  $n$ .

Another possible way to discuss the results is to identify  $T_{dc}$  with the onset temperature of the  $\alpha$  relaxation  $T_{onset}$  in these systems. So, in the high-temperature region, the ( $\alpha\beta$ ) process which should have an activated temperature dependence is measured. With decreasing temperature, the  $\alpha$  process sets in and dominates the dielectric intensity. As is known for the conventional poly(*n*-alkyl methacrylate)s, this onset temperature should shift to lower temperatures with increasing number of the spacer groups. To clarify which of the two interpretations is true requires additional investigation of experiments using specific heat spectroscopy or temperature-modulated DSC. Also dielectric investigations for samples with odd spacer lengths ( $n = 3, \dots, 11$ ) and on oriented samples will be carried out. From the theoretical side molecular dynamic simulations can be very helpful obtaining more information on both the structure and the dynamics of these systems. Such studies are in preparation.

**$\delta$  Relaxation.** As was pointed out, the  $\delta$  relaxation process is related to rotational fluctuations of the dipole component which is parallel to the mesogenic side group. The discussed mechanism is a rotational fluctuation of the whole side group around its short axis probably in a complicated multistep process. For such a process a certain microviscosity is necessary. Provided that the  $\alpha$  relaxation of the investigated polymers is related to the glass transition and so to the segmental dynamics,  $f_{p\alpha}$  is proportional to the microviscosity of the system. To abstract from that microviscosity, the temperature dependence of the ratio of the relaxation rates of the  $\alpha$  and  $\delta$  processes is discussed. In Figure 12 the ratio  $\log(f_{p\delta}/f_{p\alpha})$  is plotted versus the difference of  $T$  and the glass transition-temperature for the liquid-crystalline samples. Previously,<sup>31</sup> it was shown that this ratio is nearly a constant for isotropic comblike polymers, which is expected for isotropic melts. This is also true for the liquid-crystalline polymers above the clearing temperature. However, below this temperature a quite different behavior is observed. At the clearing temperature,  $\log(f_{p\delta}/f_{p\alpha})$  jumps to a higher value and increases further with decreasing temperature. As discussed for liquid-crystalline side-group polymeric samples, the

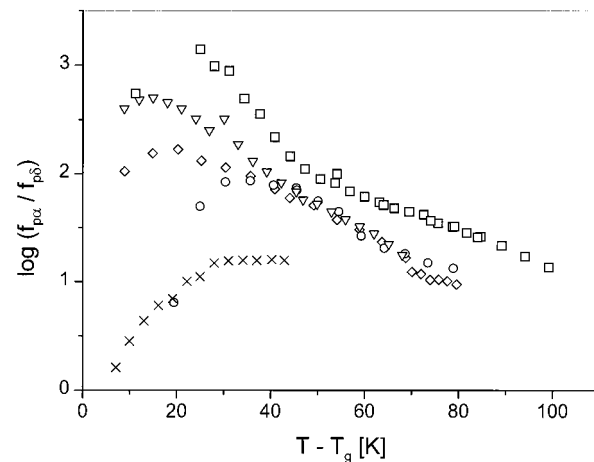


**Figure 12.** Ratio  $\log(f_{p\delta}/f_{p\alpha})$  versus  $T - T_g$  for the different liquid-crystalline samples:  $\times$ ,  $n = 2$ ;  $\circ$ ,  $n = 4$ ;  $\diamond$ ,  $n = 6$ ;  $\square$ ,  $n = 10$ .

molecular mechanism of the  $\delta$  relaxation is assumed as a complicated rotational flip-flop motion of the mesogenic groups around its short axis. If such a mechanism is true, one selected mesogenic unit has to leave one layered structure and to incorporate in another one or back in the same one. This means that the relaxation rate of the  $\delta$  process should depend on the local order of the layers. For a higher degree of order, the incorporation should be more difficult (lower relaxation rate) than that for a lower one (higher relaxation rate). Using this line of arguments, the jumplike change of  $\log(f_{p\delta}/f_{p\alpha})$  at the clearing temperature is due to the development of local order at the phase transition. With these considerations it has to be further concluded that the increase of that ratio with decreasing temperature has to be related to an increase of local order with decreasing temperature. It was further shown<sup>31</sup> that a local-order parameter can be calculated using a modified Meier and Saupe theory.<sup>25</sup> For the sample P6 this local-order parameter extracted from the dielectric measurements agrees very well with that obtained from the quadrupole splitting of the NMR spectra. This agreement is in regard to both the absolute value and the temperature dependence of the estimated order parameter and gives further evidence that developed ideas are true.

If the temperature approaches  $T_g$ , the ratio  $\log(f_{p\delta}/f_{p\alpha})$  decreases very strongly with decreasing temperature. This results from the fact that close to  $T_g$  the backbone motion becomes glassy and indicates that both relaxation processes, the  $\alpha$  and  $\delta$  relaxation freeze together. At present it seems unclear whether such cooperative processes, having such similar or close relaxation rates, could be regarded as independent relaxation processes.

**Acknowledgment.** We thank Dr. S. Czapla and Dr. U. Gessner (both of Technische Universität Berlin) for providing us with samples. A.S. thanks S. Engelschalt (ACA, Berlin-Adlershof) for many suggestions and technical support. We further thank Dr. H.-E. Carius (WITEGA, Berlin-Adlershof) for helpful discussions and support.

## References and Notes

- (1) Runt, J., Fitzgerald, J., Eds.; *Dielectric Spectroscopy of Polymeric Materials*; ACS Books: Washington, DC, 1997.

(2) Shibaev, V. P.; Platé, N.; Freidzon, Ya. S. *J. Polym. Sci. Chem.* **1979**, *17*, 1655.

(3) Finkelmann, H.; Ringsdorf, H.; Wendorff, J. H. *Makromol. Chem.* **1978**, *179*, 273.

(4) Eich, M.; Wendorff, J. H.; Reck, B.; Ringsdorf, H. *Makromol. Chem., Rapid Commun.* **1987**, *8*, 59. Eich, M.; Wendorff, J. H. *Makromol. Chem., Rapid Commun.* **1987**, *8*, 467.

(5) Kresse, H.; Talroze, R. V. *Macromol. Chem., Rapid Commun.* **1981**, *2*, 369.

(6) Kresse, H.; Kostromin, S. G.; Shibaev, V. P. *Macromol. Chem., Rapid Commun.* **1982**, *3*, 509.

(7) Kresse, H.; Trennstedt, E.; Zentel, R. *Macromol. Chem., Rapid Commun.* **1995**, *6*, 261.

(8) Haase, W.; Bormuth, F. J.; Pfeifer, M.; Jakob, E. *Ber. Bunsen-Ges. Phys. Chem.* **1991**, *95*, 1050.

(9) Haase, W.; Pranoto, H.; Bormuth, F. J. *Ber. Bunsen-Ges. Phys. Chem.* **1985**, *89*, 1229.

(10) Williams, G. Dielectric properties of polymers. In *Comprehensive Polymer Science*; Allen, G., Bevington, J. C., Eds.; Pergamon Press: Oxford, U.K., 1989; Vol. II.

(11) Kremer, F.; Schönfeld, A.; Hofmann, A.; Zentel, R.; Poths, H. *Polym. Adv. Technol.* **1992**, *3*, 249.

(12) Haws, C. M.; Clark, M. G.; Attard, G. S. Dielectric relaxation spectroscopy of liquid crystalline side chain polymers. In *Side chain liquid crystal polymers*; McArdle, C. B., Ed.; Blackie: Glasgow/London, 1989.

(13) Moscicki, J. K. Dielectric relaxation in macromolecular liquid crystals. In *Liquid crystal polymers—from structures to applications*; Collyer, A. A., Ed.; Elsevier: Amsterdam, The Netherlands, 1992.

(14) Simon, G. P. Dielectric properties of polymeric liquid crystals. In *Dielectric Spectroscopy of Polymeric Materials*; Runt, J., Fitzgerald, J., Eds.; ASC Books: Washington, DC, 1997.

(15) Schönhals, A.; Carius, H. E. Dielectric Properties of Thermotropic Polymer Liquid Crystals. In *Liquid crystal polymers—from structures to applications*; Brostow, W., Collyer, A. A., Eds.; Chapman and Hall: London, in press.

(16) Zentel, R.; Strobel, G.; Ringsdorf, H. *Macromolecules* **1985**, *18*, 960.

(17) Schönhals, A.; Wolff, D.; Springer, J. *Macromolecules* **1995**, *28*, 6254.

(18) Schönhals, A.; Wolff, D.; Springer, J. *SPIE Proc.* **1996**, *2779*, 424.

(19) Schönhals, A.; Ruhmann, R.; Thiele, Th.; Prescher, D. Molecular dynamics of liquid-crystalline side group polymers with fluorine-containing azo-chromophores. In *Photonic and optoelectronic polymers*; Jenekhe, S. A., Wynne, K. J., Eds.; ACS Symposium Series 672; American Chemical Society: Washington, DC, 1997.

(20) Attard, G. S. *Mol. Phys.* **1986**, *58*, 1087.

(21) Araki, K.; Attard, G. S.; Kozak, G. S.; Williams, G.; Gray, G. W.; Lacey, D.; Nestor, G. *J. Chem. Soc., Faraday Trans. 2* **1988**, *84*, 1067.

(22) Stickel, F.; Fischer, E. W.; Richert, R. *J. Chem. Phys.* **1995**, *102*, 6251.

(23) Anderson, P. W. *Science* **1995**, *267*, 1615.

(24) Angel, C. A. *Science* **1995**, *267*, 1924.

(25) Maier, W.; Meier, G.; Saupe, A. *Faraday Symp. Chem. Soc.* **1975**, *5*, 119.

(26) Nordio, P. L.; Rigatti, G.; Serge, U. *Mol. Phys.* **1973**, *25*, 129.

(27) Chandrasekhar, S. *Liquid Crystals*, 2nd ed.; Cambridge University Press: Cambridge, U.K., 1992.

(28) Rodekirch, G.; Rübner, J.; Zschuppe, V.; Wolff, D.; Springer, J. *Makromol. Chem.* **1993**, *194*, 1125.

(29) Wolff, D.; Rübner, J.; Springer, J., paper in preparation.

(30) Kremer, F.; Boese, D.; Meier, G.; Fischer, E. W. *Prog. Colloid Polym. Sci.* **1989**, *80*, 129. Pugh, J.; Ryan, T. *IEE Conf. Dielectric Mater. Meas. Appl.* **1979**, *177*, 404.

(31) Schönhals, A.; Gessner, U.; Rubner, J. *Makromol. Chem.* **1995**, *196*, 1671.

(32) Schlosser, E.; Schönhals, A. *Colloid Polym. Sci.* **1989**, *267*, 963.

(33) Havriliak, S.; Negami, S. *J. Polym. Sci. C* **1966**, *14*, 99.

(34) Seiberle, H.; Stille, W.; Strobel, G. *Macromolecules* **1990**, *23*, 2008.

(35) Vogel, H. *Phys. Z.* **1921**, *22*, 645. Fulcher, G. S. *J. Am. Ceram. Soc.* **1925**, *8*, 339.

(36) Garwe, F.; Schönhals, A.; Lockwenz, H.; Beiner, M.; Schroter, K.; Donth, E. *Macromolecules* **1996**, *29*, 247.

(37) Kulik, A. S.; Beckham, H. W.; Schmidt-Rohr, K.; Radloff, D.; Pawlezik, U.; Boeffel, Ch.; Spiess, H. W. *Macromolecules* **1994**, *27*, 2719.

(38) Floudas, G.; Rizos, A.; Brown, W.; Ngai, K. L. *Macromolecules* **1994**, *27*, 2719.

(39) Heijboer, J. In *Physics of Noncrystalline Solids*; Prins, J. A., Ed.; North Holland: Amsterdam, The Netherlands, 1965.

(40) Hempel, E.; Beiner, M.; Renner, T.; Donth, E. *Acta Polym.* **1996**, *47*, 525.

(41) Lipatov, Y. U.; Tsukruk, V. V.; Shilov, V. V. *Polym. Commun.* **1983**, *24*, 75.

MA9715381